Research Article J. Electrochem. Sci. Technol., 2019, 10(X), 1-11

Enhancement of Electrochemical Activity of Ni-rich $LiNi_{0.8}Mn_{0.1}Co_{0.1}O_2$ by Precisely Controlled Al_2O_3 Nanocoatings via Atomic Layer Deposition

Hari Vignesh Ramasamy[1], Soumyadeep Sinha[2], Jooyeon Park[1], Minkyung Gong[1], Vanchiappan Aravindan[3], Jaeyeong Heo[2], and Yun-Sung Lee[1,*]

[1]*Department of Advanced Chemicals and Engineering, Chonnam National University, Gwang-ju 61186, Republic of Korea.*
[2]*Department of Materials Science and Engineering, and Optoelectronics Convergence Research Center, Chonnam National University, Gwang-ju 61186, Republic of Korea*
[3]*Department of Chemistry, Indian Institute of Science Education and Research (IISER), Tirupati-517507, India.*

ABSTRACT

Ni-rich layered oxides $Li(Ni_xCo_yMn_z)O_2$ ($x + y + z = 1$) have been extensively studied in recent times owing to their high capacity and low cost and can possibly replace $LiCoO_2$ in the near future. However, these layered oxides suffer from problems related to the capacity fading, thermal stability, and safety at high voltages. In this study, we use surface coating as a strategy to improve the thermal stability at higher voltages. The uniform and conformal Al_2O_3 coating on prefabricated electrodes using atomic layer deposition significantly prevented surface degradation over prolonged cycling. Initial capacity of 190, 199, 188 and 166 mAh g^{-1} is obtained for pristine, 2, 5 and 10 cycles of ALD coated samples at 0.2C and maintains 145, 158, 151 and 130 mAh g^{-1} for high current rate of 2C in room temperature. The two-cycle Al_2O_3 modified cathode retained 75% of its capacity after 500 cycles at 5C with 0.05% capacity decay per cycle, compared with 46.5% retention for a pristine electrode, at an elevated temperature. Despite the insulating nature of the Al_2O_3 coating, a thin layer is sufficient to improve the capacity retention at a high temperature. The Al_2O_3 coating can prevent the detrimental surface reactions at a high temperature. Thus, the morphology of the active material is well-maintained even after extensive cycling, whereas the bare electrode undergoes severe degradation.

Keywords : Lithium ion battery, NCM811, Atomic layer deposition, Cathode, Thermal stability, Ultrathin coating

Received : 23 October 2018, Accepted : 18 December 2018

1. Introduction

Since the first $LiCoO_2$/graphite cell was fabricated by Sony in 1991, Li-ion batteries (LIBs) have dominated the portable energy market. To repeat its success story for large-scale applications, high-energy cathodes are necessary [1-3]. LIBs based on $Li[Ni_XCo_YAl_{1-X-Y}]O_2$ could satisfy the theoretical energy density and are used commercially in the Tesla S. Next-generation electric vehicles (EVs) are highly dependent on Ni-rich layered oxides owing to the high discharge capacity of over 220 mAh g^{-1} and the low cost, which could certainly increase the energy density to satisfy the future driving range of EVs [4,5a,5b]. However, with the increasing Ni concentration, the material is prone to several drawbacks. The trace amount of moisture in the electrolyte vigorously reacts with $LiPF_6$ and produces acidic HF, leading to dissolution of $Li(Ni_xCo_yMn_z)O_2$, especially at high temperatures [6]. Structural stability is a serious concern for these systems at high temperatures, owing to the parasitic surface reactions and the formation of an NiO-like phase from the reduction of highly reactive Ni^{4+} in the highly delithiated state and oxygen release that destabilizes the structure [7]. Micro-cracks generated from the surface of the primary particles affect the overall electrochemical performance of these layered oxides. This results in the inner core of these layered oxides being exposed to

*E-mail address: leeys@chonnam.ac.kr

DOI: https://doi.org/10.5229/JECST.2019.10.X.

unwanted side reactions, with the electrolyte thereby significantly changing the morphology after extensive cycling [8]. Micro-cracks can also generate severe degradation mechanisms, as well as other mechanisms such as phase transition. Extensive research shows that structural degradation is initiated at the surface, thereby increasing the charge-transfer resistance [9]. Hence, a stable surface/interface is necessary for the cathodes in prolonged cycle life.

To improve the electrode/electrolyte interface, different approaches have been proposed, such as surface modification [10], foreign ion substitution [11,12], the core-shell structure [13], and electrolyte additives [14]. Among these, surface modification is highly successful in mitigating the irreversible side reactions and preventing structural collapse for long cycles [10]. Thus far, metal oxides [15-21] (Al_2O_3, ZrO_2, MgO, CeO_2, ZnO, La_2O_3, TiO_2, SiO_2, etc.), phosphates [22,23a,23b] ($AlPO_4$, $FePO_4$, $Ni_3(PO_4)_2$) and fluorides [24,25] (AlF_3, CaF_2, etc.) are mostly investigated for layered oxides. Most of the aforesaid coatings were applied in a solution process. Specifically, amphoteric metal oxides such as Al_2O_3 are active HF scavengers, as follows: $Al_2O_3+6HF \rightarrow 2AlF_3+3H_2O$ [15,16]. For example Al_2O_3-coated $LiNi_{0.5}Co_{0.2}Mn_{0.3}O_2$ exhibited high capacity retention of 85% after 100 cycles compared with the pristine electrode (only 75%). Atomic layer deposition (ALD) is a non-solution-based coating technique for conformal coating of thin films and surface layers down to atomic thickness with homogeneity, a well-controllable thickness, and high device performance [26]. ALD has become an attractive technique for energy-storage applications owing to its multi-functional capabilities for developing advanced electrode materials. Another salient feature of this technique is that it can be performed at very low temperatures (less than 300°C and even room temperature) on complex structures and three-dimensional substrates [27]. This widens its spectrum of application for temperature-sensitive substrates and biomedical applications [28]. Jung et al. studied the effect of an Al_2O_3 coating applied via ALD on the cathode and anode of LIBs [29,30]. Many other studies were performed on ALD coating on the cathode, anode, and separator, and the electrochemical performance was examined [30]. Previous works on ALD coating on $LiCoO_2$ have shown positive outputs. Kim et al. applied an Al_2O_3 coating to NCM111 via ALD and thereby suppressed the charge-transfer impedance growth and capacity fading significantly for 3.0-4.5 V [31]. Yuno et al. created an outer covering of $LiAlO_2$ using the sol-gel method and decreased the capacity fading between 2.5-4.7 V [32]. Mohanty et al. coated NCM811 and NCA particles directly with Al_2O_3 and TiO_2 using ALD and studied them as pouch cells at different cutoff voltages [8]. However, only direct Al_2O_3 coating on active materials before electrode fabrication has been done thus far. This hinders the Li^+ and electron conduction, resulting in poor kinetics at a high input current. Further, the thickness of the Al_2O_3 coating can have a significant effect on the electrochemical performance, and reports suggest that an optimized coating thickness is mandatory.

We studied the effect of different numbers of cycles of ALD Al_2O_3 coating on prefabricated NCM811 electrodes in the voltage range of 2.8-4.3 V at room temperature and a high temperature (50°C). Apparently, the Al_2O_3 coating improved both the initial capacity and the high-rate capability in both the room-temperature and elevated-temperature conditions. At the high temperature, the optimized ALD cycle (2) greatly improved the capacity retention to 75% under cycling at a rate of 5C up to 500 cycles. These results are meaningful for the development of NCM811 as a future cathode for EVs.

2. Experimental

The electrochemical performance of all samples was studied using CR2032 coin cells, which were assembled inside a glovebox filled with ultrapure Ar, in which the O_2 and H_2O levels were maintained below 1 ppm. Commercial NCM811 (Ecopro, South korea) was used as a cathode, and Li metal was used as the anode. Whatman glass-fiber filter paper was used as a separator, and 1 M $LiPF_6$ in EC:DMC (1:1) was used as the electrolyte solution. Each cathode consisted of 2.5 mg of the active material mixed with 0.5 mg of Ketjen black and 0.5 mg of Teflonized acetylene black (TAB-2). The slurry obtained with the assistance of ethanol was pressed on a stainless-steel current collector (200 mm^2 area) and dried in a vacuum oven at 160°C for 4 h before cell fabrication. Charge/discharge studies were performed in the voltage range of 2.8-4.3 V with varying current rates of 85, 170, 340, 650, and 1,700 mA g^{-1} using an Arbin BT-2000 battery testing system. Cyclic voltammetry

and impedance measurements were conducted using an electrochemical analyzer (SP-150, Biologic, France.)

A thin layer of Al_2O_3 film was deposited in a laminar-flow-type thermal ALD reactor (NCD, Lucida D100, Korea) on the prefabricated electrodes at the substrate temperature of 150°C using trimethylaluminum (TMA) and de-ionized-H_2O as the Al and O sources, respectively. The TMA and H_2O sources were kept at 10°C throughout the deposition process. A continuous flow of N_2 gas (50 sccm) was used as the carrier gas and also for the purging during the deposition process. The reaction scheme for one Al_2O_3 ALD cycle was set as follows: 0.5 s pulsing of TMA, 20 s purging of N_2, 0.5 s pulsing of H_2O, and 20 s purging of N_2. The repetition of the aforementioned sequence for two, five, and 10 cycles resulted in different thicknesses of the Al_2O_3 coating on the cathode materials. Hereinafter, the electrodes are denoted as NCM811-0c, NCM811-2c, NCM811-5c, and NCM811-10c, respectively.

The crystal structures were characterized via X-ray diffraction (XRD; Cu K_a radiation, Rint 1000, Rigaku, Japan) in the 2θ range of 5°-90°. The lattice parameters were determined by Rietveld refinement using the GSAS software. The particle morphology, elemental composition, and internal structure were evaluated using field-emission scanning electron microscopy (FE-SEM, S-4700, Hitachi, Japan), energy-dispersive X-ray spectroscopy, and high-resolution transmission electron microscopy (HR-TEM; JEM-2000, EX-II, JEOL, Japan), respectively. The stoichiometry was determined via inductively coupled plasma atomic emission spectroscopy analysis (Perkin Elmer, OPTIMA 8300, USA). XPS measurements (Multilab 2000, UK) were performed to determine the chemical oxidation sates of Mn, Ni, and Co on the compound surface.

3. Result and Discussion

Fig. 1 shows the structural and morphological properties of the NCM811 obtained from Ecopro (Korea) using XRD, FE-SEM, and TEM. As shown in Fig. 1(a), the well-defined XRD peaks represent the hexagonal α-$NaFeO_2$ structure with the R-3m space group [33]. The peaks are further indexed using the hexagonal α-$NaFeO_2$ structure. The absence of additional peaks and the splitting of (006)/(102) and (108)/(110) denote the phase purity of the sample, along with the well-defined layered structure. Fig. 1(b) shows the morphology of the single

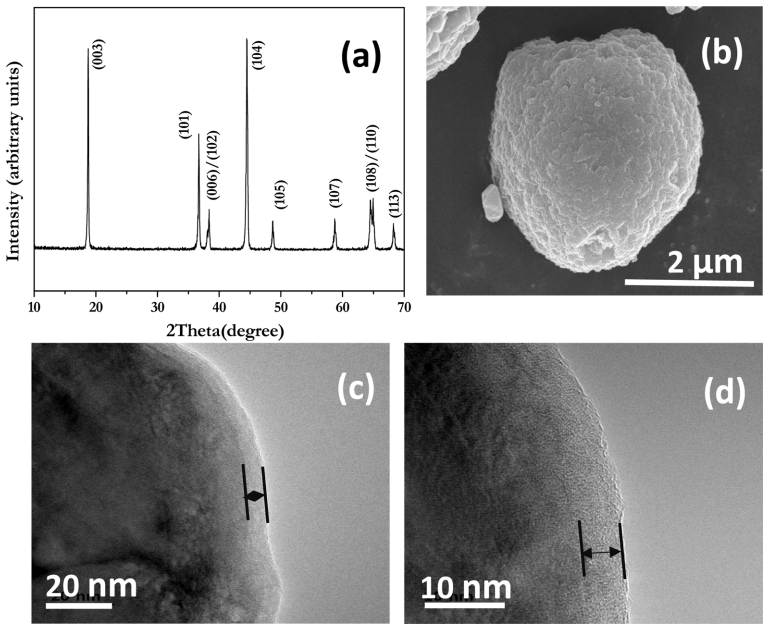

Fig. 1. XRD peaks of $LiNi_{0.8}Co_{0.1}Mn_{0.1}O_2$ obtained from Ecopro (Korea). (b) FE-SEM image of NCM811 with a spherical morphology (c and d). HR-TEM images of 50-cycle ALD Al_2O_3-modified particles.

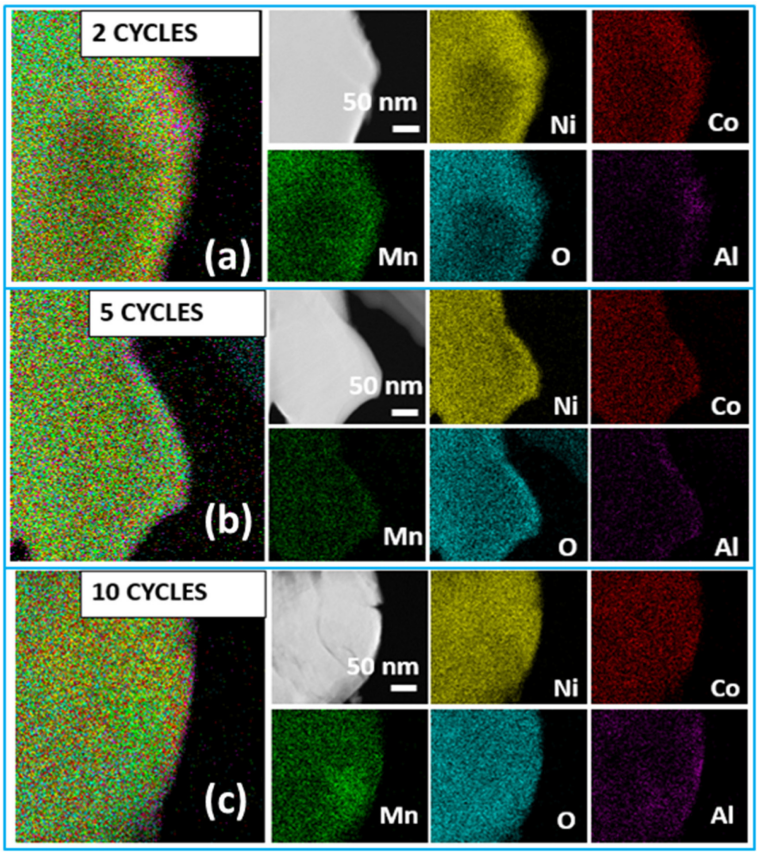

Fig. 2. TEM elemental mapping of $LiNi_{0.8}Co_{0.1}Mn_{0.1}O_2$ with two, five, and 10 cycles of ALD Al_2O_3 modification.

particle of as-obtained NCM811 with a distinct spherical shape as an advantage for a high tap density and an aid to formulate the quality electrodes. The uniform and conformal coating of ALD Al_2O_3 is confirmed by the magnified TEM image, as shown in Figs. 1(c and d). For the purpose of characterization, the electrodes are fabricated with less conductive C and coated with different thicknesses of ALD Al_2O_3. The particles at the surface of the cathode are removed properly and used for further analysis. For a 50-cycle ALD-coated electrode, an amorphous coating layer approximately 5 nm thick is clearly visible. This uniform coating protects the cathodes from electrolyte attack and improves the stability. Elemental distribution mapping was performed to confirm the distribution of individual elements over the surface. Fig. 2 confirms that Ni, Mn, Co and O are uniformly distributed over the particle. Further, the TEM elemental mapping of the 50-cycle ALD coating is presented in Fig. s1. A clear Al mapping is visible near the edge, confirming the uniformity of the Al_2O_3 coating corresponding to that observed in the TEM image.

Fig. 3(a) shows the charge-discharge curves of NCM811 electrodes modified with different thicknesses of the Al_2O_3 coating at a rate of 0.2C (1C = 200 mA g^{-1}) within the voltage window of 2.8-4.3 V. It provides an initial capacity of ~190, ~199, ~188, and ~166 mAh g^{-1} for pristine, 2, 5, and 10 cycles of ALD coating. It is clear that the two-cycle ALD-coated electrode has a higher capacity than the pristine electrode. Further, the capacity is found to decrease linearly with the increasing coating thickness. Hence, an optimized coating thickness is necessary to realize better electrochemical performance. In the first place, an inactive protective matrix at the interface effectively prevents the cathode from direct contact with the electrolyte species and suppresses the side reactions [16]. Once the thickness of coating layer exceeds the threshold

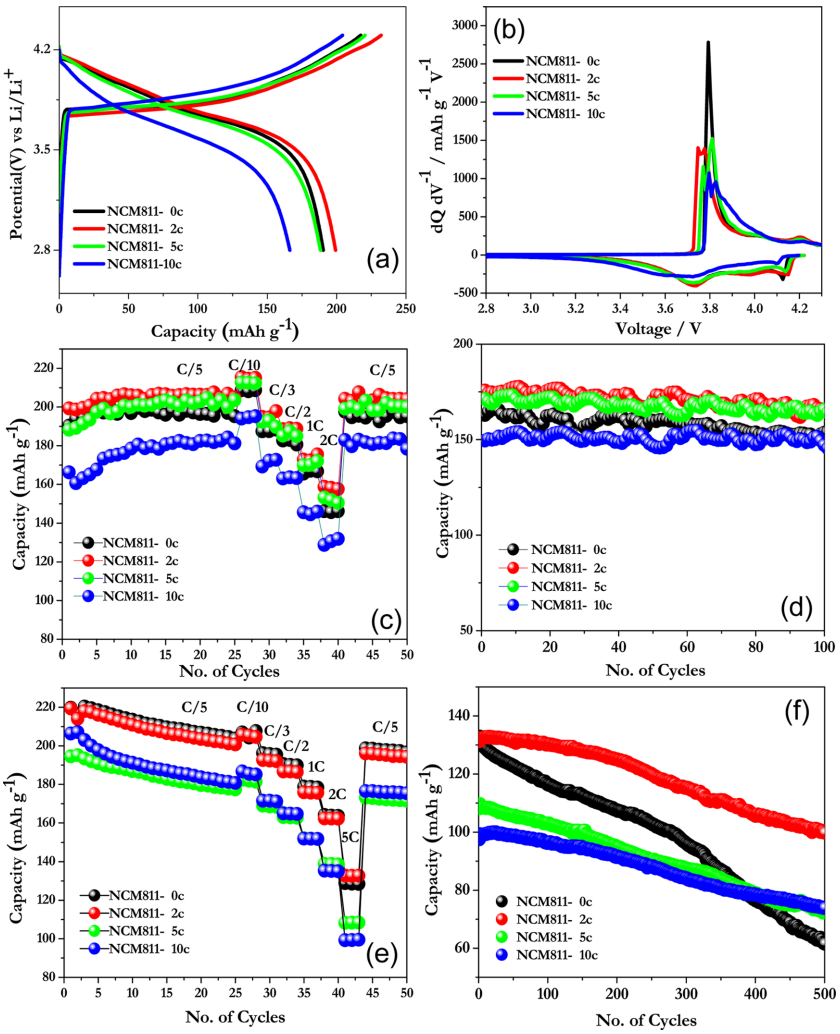

Fig. 3. (a, b) Charge–discharge and differential capacity plot of ALD-modified NCM811 at room temperature (0.2 C rate). (c) Rate capability studies and (d) cycling profiles of Al_2O_3-modified NCM811 at room temperature at a rate of 1 C. (e) Rate performance of ALD-modified NCM811 electrodes at 50°C. (f) Cycling stability of Al_2O_3-modified NCM811 electrodes at a rate of 5 C in elevated-temperature conditions.

value, the Li^+ ion and electron transport kinetics are severely affected [34a]. This property is material-sensitive and varies with different materials. The intensity ratio of (003)/(104) is an important factor to determine the degree of disorder in the layered oxides. It has been reported that, Al_2O_3 and $AlPO_4$ surface coating resulted in increased (003)/(104) ratio for nickel rich layered oxides by preventing the cation mixing and having a much ordered surface structure. This results in lower activation barrier for diffusion of lithium in the layered structure. Thus optimized Al_2O_3 coating decreases the activation energy at the interface, thereby increasing the Li^+ ion migration, leading to a high capacity [35]. Initial few cycles of ALD coating leads to partial coverage of Al at the interstitial sites of cathode electrode surface. The Aluminium ions from the Trimethyl Aluminium (TMA) precursor is tend to bond with the surface sites of the active materials and results in the graded incorporation of the Al into the structure through highly reactive and self-limiting chemistry. This justifies the improved electro-

chemical performance of 2 cycle ALD modified NCM811 electrode at room temperature and elevated temperature. It also provides more channels for Li^+ ion migration [36,46]. The corresponding differential capacity plot is given in Fig. 3(b). Three pairs of redox peaks are present in the voltage window of 2.8-4.3V for the bare electrode without the ALD coating. The sharp peaks centered at 3.75 V correspond to Ni^{2+}-Ni^{4+}, and another broad peak at 4.2 V correspond to Co^{3+}-Co^{4+}, along with other structural transitions similar to those of NCM811 [15]. For two-cycle ALD-modified electrodes, the $Ni^{2+/4+}$ peaks are shifted to a lower voltage, and the separation between the peaks is minimized. This implies that the polarization and impedance are reduced. When the coating thickness is increased, the polarization is increased, resulting from the Li^+/electron migration clearly reflected in the interfacial charge-transfer resistance derived from the impedance plot.

Rate capability studies were performed at different current densities between 2.8 and 4.3 V for pristine and ALD-modified electrodes (Fig. 3(c)). The NCM811 electrode without any surface modifications delivered 190, 208, 188, 183, 167, and 146 mAh g^{-1}, at rates of 0.2, 0.1, 0.3, 0.5, 1, and 2C, respectively. When the cells were cycled back to a lower current of 0.2C, the electrode still delivered a capacity of 195 mAh g^{-1}, showing good recovery characteristics. The discharge capacity decreases with the increasing current density owing to the lower diffusion rate of the cathode electrodes at a higher current rate. The rate performance of NCM811 with two-cycle Al_2O_3 coating was enhanced with 199, 214, 195, 189, 172, and 158 mAh g^{-1} for the aforementioned current rates, and the electrode exhibited a recovery capacity of 203 mAh g^{-1} when cycled at the rate of 0.2C. NCM811 with five cycles of ALD coating also gives a higher capacity than the pristine electrode, and as the thickness increases to 10 cycles, the rate performance degradation increases. This is because a thin ALD coating accelerates the formation of the stable interfacial layer with a more desirable structure, resulting in improved electrochemical kinetics [37]. In this case, the Al_2O_3 coating is directly applied on the prefabricated electrode without impeding the electrical conducting pathways between the active material and conductive C. As the thickness of the coating increases, the movement of Li^+ is impeded, resulting in a poor rate capability [34]. Cyclic stability is an important factor for increasing the driving range of EVs. Here, the cells were tested at the rate of 1C between 2.8-4.3 V for 100 cycles (Fig. 3(d)). The pristine electrode delivered a capacity of 163 mAh g^{-1} at a rate of 1C rate and retained 151 mAh g^{-1} after 100 cycles with a capacity retention of 92.56%. In comparison, the two-cycle Al_2O_3-coated cathodes delivered 176 mAh g^{-1} and retained a capacity of 165 mAh g^{-1} (93.08%) after 100 cycles. The stability of cathodes significantly increases with a higher coating thickness, at the expense of the capacity. The five- and ten-cycle ALD-coated electrode delivered a low capacity of 171 and 149 mAh g^{-1} and retained 96.75 and 98.45%, respectively, after 100 cycles. This results clearly show the improvement in the electrochemical performance of the ALD-modified Ni-rich cathodes. Li et al. applied an ALD coating to $LiCoO_2$ electrodes using different metal oxides and confirmed the positive role of Al_2O_3 in improving the capacity retention compared with other oxides [15-17].

To assess the influence of surface encapsulation, electrodes with different Al_2O_3 thicknesses were cycled at an elevated temperature (50°C) in the same potential window of 2.8-4.3 V. Fig. 3(e) presents the rate performance at different current rates of 0.2, 0.1, 0.3, 0.5, 1, 2, and 5C. The conformal coating of Al_2O_3 appears to have no significance at the lower current rates, as the pristine electrode delivered a higher capacity regardless of the applied current rate. However, an obvious difference is noted at the rate of 5C: the two-cycle ALD coating exhibits a higher capacity than the other coating cycles. Further cyclic stability at this 5C rate is extended for 500 cycles between 2.8 and 4.3 V. Electrodes without the ALD coating exhibit drastic capacity fading and retain only 46.59% after 500 cycles. In contrast, the electrode with a very thin Al_2O_3 coating (two cycles) has higher capacity retention of 76.33%. An increased thickness of 10 cycles of ALD yields better capacity retention, but at the expense of a low specific capacity, as the thick layer could hinder the diffusion of Li ions at very high charge-discharge rate [34]. The capacity fading of bare electrodes occurs for a variety of reasons: (i) there are deleterious side reactions when the electrodes are charged to a higher operating voltage of 4.3 V, at which most of the non-aque-

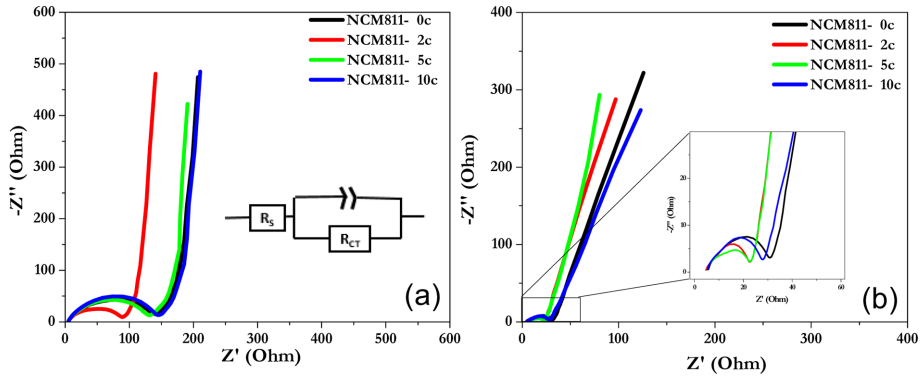

Fig. 4. EIS spectra of ALD Al_2O_3-modified electrodes (a) before (inset shows the equivalent circuit) and (b) after cycling at a rate of 1 C at room temperature for 100 cycles.

ous electrolytes are easily oxidized [38], (ii) the presence of highly reactive Ni^{4+} at the end of the charge could fasten the electrolyte decomposition [39], (iii) the migration of transition Ni^{4+} metal ions from octahedral 3a sites to Li sites (octahedral 3b) at delithiated state causes irreversible structural change to the rock salt and spinal phase, hindering Li^+ ion migration [40], (iv) the fluorinated anion species in the electrolyte corrodes the interfacial layer, resulting in decomposition products such as LiF, Li_xPF_y, and $Li_xPO_yF_z$, along with other gaseous products such as CO_2 and alkanes [41a], (v) the continuous development of microstrain in the unmodified sample results in loss of crystallinity and thereby capacity fading [41b,23b], (vi) Over-prolonged cycling can aggravate the dissolution of transition metals, especially Mn. All the aforementioned mechanisms are further aggravated at elevated temperature conditions and cause degradation of the electrodes [42]. Whereas the electrodes with surface modification maintains good structural stability and good capacity retention.

Figs. 4 (a, b) show the electrochemical impedance spectroscopy (EIS) results for NCM811 electrodes coated with different numbers of cycles of Al_2O_3 coating using ALD. The EIS spectra clearly illustrate the relationship between the impedance and the thickness of the cathode interface coated with Al_2O_3. Each spectrum has a single semicircle from the high-frequency region to the medium-frequency region, denoting the charge-transfer resistance (R_{ct}) mainly at the electrode-electrolyte interface. [43a, 43b]. To have a quantitative idea of the resistance, the obtained spectra are fitted with an equivalent circuit, as shown in the inset of Fig. 4(a), which has R_s the solution resistance and R_{ct} the charge transfer resistance. The results indicate that NCM811 coated with two cycles of ALD has a lower charge-transfer resistance than the other coating cycles. Thus, an optimized thin ALD coating can act as a protective matrix for the cathode without hindering the movement of ions and electron across the interface. The lower charge-transfer resistance of the coated sample is due to the protective effect of Al_2O_3 before exposure to O_2 and H_2O before fabrication [44a]. Impedance is also measured after cycling to assess the stability of the electrodes. The NCM811 electrode tested for 100 cycles at room temperature at 1 C rate was considered. It has similar type of semicircle denoting R_{ct}. The R_{ct} is significantly reduced for all the cells after cycling because of the greater interaction of the electrolyte with the active material after cycling. Nonetheless, the electrode with two-cycle Al_2O_3 coating exhibits better performance than the others. In general, all surface modified cathodes have lower charge transfer resistance. This is due to the role of surface species resulting from the extensive cycling at higher voltages. The acidic species like HF generated during cycling can act as a catalyst in polymerizing the Alkyl carbonates with the surface species formed during cycling. Also it has a strong influence on the impedance behavior as seen in figure. 4b [44b].

To reveal the robustness of the ALD Al_2O_3 coating in alleviating the formation of cracks caused by the structural degradation and the volume contraction and expansion during the continuous charge–discharge process, we dismantled the coin cells and ana-

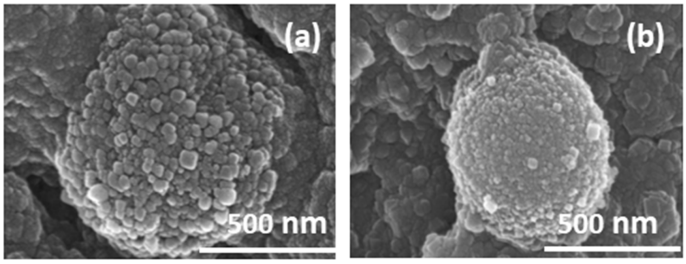

Fig. 5. FE-SEM images of the NCM811 electrode after 500 cycles at a high temperature (50°C): (a) pristine electrode and (b) Al_2O_3-coated electrode/

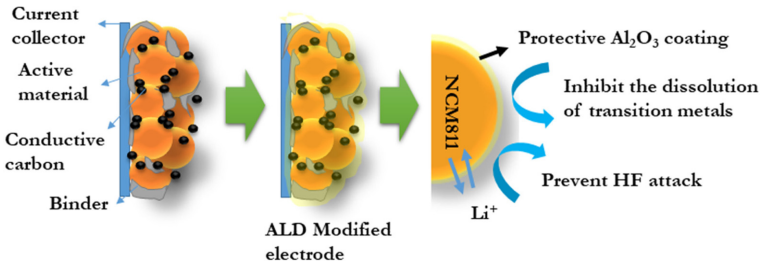

Fig. 6. Schematic of ALD Al_2O_3-modified NCM811 electrode

lyzed the particle morphology of both the modified and pristine electrodes, and the corresponding FE-SEM image is shown in Fig. 5. The spherical morphology of the NCM811 is well-preserved in the ALD-modified cathode (Fig. 5b). The cycled pristine electrodes have extensive and visible cracks (Fig. 5a). The secondary aggregate particles are highly disintegrated, leading to more penetration of electrolyte to the bulk and accelerate structural degradation along with other surface side reactions resulting in the dissolution of the transition metals in the delithiated state [42]. As analyzed by Wang et al. higher fraction of particles are subjected to severe microstrain, fracture and defects during cycling. All these lead to capacity fading over long cycles at a high temperature [45]. In contrast, the micro-cracks due to the anisotropic volume expansion are not visible even after 500 cycles at a rate of 5C, exhibiting excellent cycle stability, as indicated by the electrochemical performance. This is because the Al_2O_3 acts as a flexible matrix to accommodate the volume change and prevents the reaction of the electrode with HF generated in the electrolyte, as well as metal dissolution [15]. A schematic depicting the interfacial modification using ALD Al_2O_3 and its function as a protective covering is provided in Fig. 6.

5. Conclusions

We successfully modified the interface of the NCM811 cathode by Al_2O_3 using ALD. High capacity of 190, 199, 188 and 166 mAh g^{-1} is obtained for pristine, 2, 5 and 10 cycles of ALD coated samples at 0.2C and maintains 145, 158, 151 and 130 mAh g^{-1} for high current rate of 2C in room temperature. The Al_2O_3-modified cathode results in 76.33% capacity retention even after 500 cycles (5C) at an elevated temperature, whereas the pristine electrode exhibits only 46.59%. Electrochemical results showed that surface engineering could significantly mitigate the detrimental side reactions along the interface and thereby improve the stability and rate performance of NCM811 under both room-temperature and elevated-temperature conditions. Post-mortem analysis clearly showed the beneficial effect of surface modification with Al_2O_3 via ALD. This clearly indicates that the conformal surface modification not only enhances the electrochemical profile but also prevents the structural degradation of cathodes under ambient-temperature and elevated-temperature conditions. This could be a significant step towards realizing high-energy cathode materials for practical applications using conformal surface coating with ALD.

Acknowledgement

This study was financially supported by Chonnam National University, 2016

References

[1] D. Andre, S. J. Kim, P. Lamp, S. F. Lux, F. Maglia, O. Paschos and B. Stiaszny, Future Generations of Cathode Materials: an Automotive Industry Perspective, *J. Mater. Chem. A*, **2015**, *3*, 6709-6732.

[2] D. Jang, K. Palanisamy, Y. Kim, and W.S. Yoon, Structural and Electrochemical Properties of Doped $LiFe_{0.48}Mn_{0.48}Mg_{0.04}PO_4$ as Cathode Material for Lithium ion Batteries, *J. Electrochem. Sci. Technol.*, **2013**, *3(3)*, 102-107.

[3] J. Kim, N. Go, H. Kang, A. Tron, and J. Mun, Effect of Fluoroethylene Carbonate in the Electrolyte for $LiNi_{0.5}Mn_{1.5}O_4$ Cathode in Lithium-ion Batteries, *J. Electrochem. Sci. Technol*., **2017**, *8(1)*, 53-60.

[4] M. Latifatu, C. Y. Bon, K. S. Lee, L. Hamenu, Y. Il Kim, Y. J. Lee, Y. M. Lee, and J. M. Ko, Structural Effect of Conductive Carbons on the Adhesion and Electrochemical Behavior of $LiNi_{0.4}Mn_{0.4}Co_{0.2}O_2$ Cathode for Lithium Ion Batteries., *J. Electrochem. Sci. Technol*., **2018**, *9(4)*, 330-338.

[5a] J. W. Lee and Y. J. Park, Enhanced Cathode/Sulfide Electrolyte Interface Stability Using an Li_2ZrO_3 Coating for All-Solid-State Batteries, *J. Electrochem. Sci. Technol*., **2018**, *9(3)*, 176-183.

[5b] G. W. Yoo and J. T. Son, Improvement of Electrochemical Properties and Thermal Stability of a Ni-rich Cathode Material by Polypropylene Coating, *J. Electrochem. Sci. Technol*., **2016**, *7(2)*, 179-184.

[6] Y. K. Sun, Z. Chen, H. J. Noh, D. J. Lee, H. G. Jung, Y. Ren, S. Wang, C. S. Yoon, S. T. Myung and K. Amine, Nanostructured High-Energy Cathode Materials for Advanced Lithium Batteries, *Nat. Mater*, **2012**, 11, 942-947.

[7] D. Song, P. Hou, X. Wang, X. Shi and L. Zhang, Understanding the Origin of Enhanced Performances in Core−Shell and Concentration-Gradient Layered Oxide Cathode Materials, *ACS Appl. Mater. Interfaces*, **2015**, *7*, 12864-12872.

[8] D. Mohanty, K. Dahlberg, D. M. King, L. A. David, A. S. Sefat, D. L. Wood, C. Daniel, S. Dhar, V. Mahajan, M. Lee and F. Albano, Modification of Ni-Rich FCG NMC and NCA Cathodes by Atomic Layer Deposition: Preventing Surface Phase Transitions for High-Voltage Lithium-Ion Batteries, *Scientific Reports*, **2016**, *6*, 26532.

[9] S. K. Jung, H. Gwon, J. Hong, K. Y. Park, D. H. Seo, H. Kim, J. Hyun, W. Yang and K. Kang, Understanding the Degradation Mechanisms of $LiNi_{0.5}Co_{0.2}Mn_{0.3}O_2$ Cathode Material in Lithium Ion Batteries, *Adv. Energy Mater*, **2014**, *4*, 1300787.

[10] L. A. Riley, S. V. Atta, A. S. Cavanagh, Y. Yan, S. M. George, P. Liu, A. C. Dillon, S. H. Lee, Electrochemical Effects of ALD Surface Modification on Combustion Synthesized $LiNi_{1/3}Mn_{1/3}Co_{1/3}O_2$ as a Layered-Cathode Material, *J. Power Sources*, **2011**, *196*, 3317-3324.

[11] S. Wolff-Goodrich, F. Lin, I. M. Markus, D. Nordlund, H. L. Xin, M. Asta and M. M. Doeff, Tailoring the Surface Properties of $LiNi_{0.4}Mn_{0.4}Co_{0.2}O_2$ by Titanium Substitution for Improved High Voltage Cycling Performance, *Phys. Chem. Chem. Phys*, **2015**, *17*, 21778-21781.

[12] K. R. Prakasha, M. Sathish, P. Bera and A. S. Prakash, Mitigating the Surface Degradation and Voltage Decay of $Li_{1.2}Ni_{0.13}Mn_{0.54}Co_{0.13}O_2$ Cathode Material through Surface Modification Using Li_2ZrO_3, *ACS Omega*, **2017**, *2*, 2308-2316.

[13] J. Zhang, Z. Yang, R. Gao, L. Gu, Z. Hu and X. Liu, Suppressing the Structure Deterioration of Ni-Rich $LiNi_{0.8}Co_{0.1}Mn_{0.1}O_2$ through Atom-Scale Interfacial Integration of Self-Forming Hierarchical Spinel Layer with Ni Gradient Concentration, *ACS Appl. Mater. Interfaces*, **2017**, *9*, 29794-29803.

[14] W. Zhao, G. Zheng, M. Lin, W. Zhao, D. Li, X. Guan, Y. Ji, G. F. Ortiz, Y. Yang, Toward a Stable Solid-Electrolyte-Interfaces on Nickel-Rich Cathodes: $LiPO_2F_2$ Salt-Type Additive and its Working Mechanism for $LiNi_{0.5}Mn_{0.25}Co_{0.25}O_2$ Cathodes, *J. Power Sources*, **2018**, *380*, 149-157.

[15] F. Schipper, H. Bouzaglo, M. Dixit, E. M. Erickson, T. Weigel, M. Talianker, J. Grinblat, L. Burstein, M. Schmidt, J. Lampert, C. Erk, B. Markovsky, D. T. Major and D. Aurbach, From Surface ZrO_2 Coating to Bulk Zr Doping by High Temperature Annealing of Nickel-Rich Lithiated Oxides and Their Enhanced Electrochemical Performance in Lithium Ion Batteries, *Adv. Energy Mater*, **2018**, *8*, 1701682.

[16] Y. Su, S. Cui, Z. Zhuo, W. Yang, X. Wang and F. Pan, Enhancing the High-Voltage Cycling Performance of $LiNi_{0.5}Mn_{0.3}Co_{0.2}O_2$ by Retarding Its Interfacial Reaction with an Electrolyte by Atomic-Layer-Deposited Al_2O_3, *ACS Appl. Mater. Interfaces*, **2015**, *7*, 25105-25112.

[17] E. Zhecheva, R. Stoyanova, G. Tyuliev, K. Tenchev, M. Mladenov, S. Vassilev, Surface Interaction of $LiNi_{0.8}Co_{0.2}O_2$ Cathodes with MgO, *Solid State Sciences*, **2003**, *5*, 711-720.

[18] K. Liu, G. L. Yang, Y. Dong, T. Shi, L. Chen, Enhanced Cycling Stability and Rate Performance of $Li[Ni_{0.5}Co_{0.2}Mn_{0.3}]O_2$ by CeO_2 Coating at High Cut-Off Voltage, *Journal of Power Sources*, **2015**, *281*, 370-377.

[19] S. M. Lee, S. H. Oh, J. P. Ahn, W. I. Cho, H. Jang, Electrochemical Properties of ZrO_2-Coated $LiNi_{0.8}Co_{0.2}O_2$ Cathode Materials, *J. Power Sources*, **2006**, *159*, 1334-1339.

[20] W. Cho, S. M. Kim, J. H. Song, T. Yim, S. G. Woo, K. W. Lee, J. S. Kim, Y. J. Kim, Improved Electrochemical

and Thermal Properties of Nickel Rich $LiNi_{0.6}Co_{0.2}Mn_{0.2}O_2$ Cathode Materials by SiO_2 Coating, *J. Power sources*, **2015**, *282*, 45-50.

[21] D. Bhuvaneswari, G. Babu, N. Kalaiselvi, Effect of Surface Modifiers in Improving the Electrochemical Behavior of $LiNi_{0.4}Mn_{0.4}Co_{0.2}O_2$ Cathode, *Electrochimica Acta*. **2013,** *109*, 684-693.

[22] T. N. Phan, M. K. Gong, R. Thangavel, Y. S. Lee, C. H. Ko, Ordered mesoporous carbon CMK-8 cathodes for high-power and long-cycle life sodium hybrid capacitors, *J. Alloys Compd*, **2017,** *728*, 1305-1314.

[23a]D. J. Lee, B. Scrosati, Y. K. Sun, $Ni_3(PO_4)_2$-Coated $Li[Ni_{0.8}Co_{0.15}Al_{0.05}]O_2$ Lithium Battery Electrode with Improved Cycling Performance at 55°C, *J. Power Sources*, **2011**, *196*, 7742-7746.

[23b]Z. Wang, C. Wu, L. Liu, F. Wu, L. Chen, X. Huang, Electrochemical evaluation and structural characterization of commercial $LiCoO_2$ surfaces modified with MgO for Lithium Ion Batteries, *J. Electrochem. Soc*, **2002**, *149*, A466-A471.

[24] H. B. Kim, B. C. Park, S. T. Myung, K. Amine, J. Prakash, Y. K. Sun, Electrochemical and Thermal Characterization of AlF_3-Coated $Li[Ni_{0.8}Co_{0.15}Al_{0.05}]O_2$ Cathode in Lithium-ion Cells, *J. Power Sources*, **2008**, *179*, 347-350.

[25] Y. K. Sun, S. T. Myung, B. C. Park and H. Yashiro, Improvement of the Electrochemical Properties of $Li[Ni_{0.5}Mn_{0.5}]O_2$ by AlF_3 Coating, *J. Electrochem. Soc*, **2008**, *155*, A705-A710.

[26] S.M. George, Atomic Layer Deposition: An Overview, *Chem. Rev*, **2010**, *110*, 111-131.

[27] L. Wen, M. Zhou, C. Wang, Y. Mi, Y. Lei, Nanoengineering Energy Conversion and Storage Devices via Atomic Layer Deposition, *Adv. Energy Mater*, **2016**, *6*,1600468.

[28] X. Meng, Atomic-scale Surface Modifications and Novel Electrode Design for High-performance Sodium-ion Batteries via Atomic Layer Deposition, *J. Mater. Chem. A*, **2017**, *5*, 10127-10149.

[29] Y.S. Jung, A.S. Cavanagh, L.A. Riley, S.H. Kang, A.C. Dillon, M.D. Groner, S.M. George, S.H. Lee, Ultrathin direct atomic layer deposition on composite electrodes for highly durable and safe Li-Ion batteries, *Adv. Mater*, **2010**, *22*, 2172-2176.

[30] Y.S. Jung, A.S. Cavanagh, A.C. Dillon, M.D. Groner, S.M. George, S.-H. Lee, Enhanced Stability of $LiCoO_2$ Cathodes in Lithium-Ion Batteries Using Surface Modification by Atomic Layer Deposition, *J. Electrochem. Soc*, **2010**, *157*, A75-A81.

[31] J. W. Kim, J. J. Travis, E. Hu, K. W. Nam, S. C. Kim, C. S. Kang, J. H. Woo, X. Q. Yang, S. M. George, K. H. Oh, S. J. Cho, S. H. Lee, Unexpected High Power Performance of Atomic Layer Deposition Coated $Li[Ni_{1/3}Mn_{1/3}Co_{1/3}]O_2$ Cathodes, *J. Power Sources*, **2014**, *254*, 190-197.

[32] A. Yano, S. Aoyama, M. Shikano, H. Sakaebe, K. Tatsumi and Z. Ogumi, Surface Structure and High-Voltage Charge/Discharge Characteristics of Al-Oxide Coated $LiNi_{1/3}Co_{1/3}Mn_{1/3}O_2$ Cathodes, *J. Electrochem. Soc*, **2015**, *162*, A3137-A3144.

[33] W. Liu, X. Le, D. Xiong, Y. Hao, J. Li, H. Kou, B. Yan, D. Li, S. Lu, A. Koo, K. Adair, X. Sun, Significantly Improving Cycling Performance of Cathodes in Lithium Ion Batteries: The Effect of Al_2O_3 and $LiAlO_2$ Coatings on $LiNi_{0.6}Co_{0.2}Mn_{0.2}O_2$, *Nano Energy*, **2018**, *44*, 111-120.

[34] S. T. Myung, K. Izumi, S. Komaba, Y. K. Sun, H. Yashiro and N. Kumagai, Role of Alumina Coating on Li-Ni-Co-Mn-O Particles as Positive Electrode Material for Lithium-Ion Batteries, *Chem. Mater.*, **2005**, *17*, 3695-3704.

[35] J. Kang and B. Han, First-Principles Study on the Thermal Stability of $LiNiO_2$ Materials Coated by Amorphous Al_2O_3 with Atomic Layer Thickness, *ACS Appl. Mater. Interfaces*, **2015**, *7*, 11599-11603.

[36] Y. Zhao, J. Li and J. R. Dahn, Interdiffusion of Cations from Metal Oxide Surface Coatings into $LiCoO_2$ during Sintering, *Chem. Mater*, **2017**, *29*, 5239-5248.

[37] W. Lu, L. Liang, X. Sun, X. Sun, C. Wu, L. Hou, J. Sun and C. Yuan, Recent Progresses and Development of Advanced Atomic Layer Deposition towards High-Performance Li-Ion Batteries, *Nanomaterials*, **2017**, *7*, 325.

[38] G. Cherkashinin, M. Motzko, N. Schulz, T. Spath and W. Jaegermann, Electron Spectroscopy Study of $Li[Ni,Co,Mn]O_2$/Electrolyte Interface:Electronic Structure, Interface Composition, and Device Implications, *Chem. Mater*, **2015**, *27*, 2875-2887.

[39] P. Y. Hou, L. Q. Zhang and X. P. Gao, A High-Energy, Full Concentration-Gradient Cathode Material with Excellent Cycle and Thermal Stability for Lithium Ion Batteries, *J. Mater. Chem. A*, **2014**, *2*, 17130-17138.

[40] S. Hwang, D. H. Kim, K. Y. Chung and W. Chang, Understanding Local Degradation of Cycled Ni-Rich Cathode Materials at High Operating Temperature for Li-Ion Batteries, *Appl. Phys. Lett,* **2014**, *105*, 103901.

[41a]R. Younesi, A. S. Christiansen, R. Scipioni, D. T. Ngo, S. B. Simonsen, K. Edstrom, J. Hjelm and P. Norby, Analysis of the Interphase on Carbon Black Formed in High Voltage Batteries, *J. Electrochem. Soc*, **2015**, *162*, A1289-A1296.

[41b]A. M. Kannan, A. Manthiram, Surface Chemically Modified $LiMn_2O_4$ Cathodes for Lithium Ion Batteries, *Electrochemical and Solid state letters*, **2002**, *5(7)*, A167-A169.

[42] S. Watanabe, M. Kinoshita, T. Hosokawa, K. Morigaki, K. Nakura, Capacity Fade of $LiAl_yNi_{1-x-y}Co_xO_2$ Cathode for Lithium-Ion Batteries During Accelerated Calendar and Cycle Life Tests (Surface Analysis of $LiAl_yNi_{1-x-y}Co_xO_2$ Cathode After Cycle Tests in Restricted Depth of Discharge Ranges), *Journal of Power Sources*, **2014**, *258*, 210-217.

[43a]H. V. Ramasamy, K. Kaliyappan, R. Thangavel, V. Aravindan, K. Kang, D. U. Kim, Y. Park, X. Sun Y. S. Lee, Cu-doped P2-Na0.5Ni0.33Mn0.67O2 encapsulated with MgO as a novel high voltage cathode with enhanced Na-storage properties, *J. Mater. Chem. A,* **2017**, *5*, 8408.

[43b]H. V. Ramasamy, K. Kaliyappan, R. Thangavel, W. M. Seong, K. Kang, Z. Chen, Y. S. Lee, Efficient Method of Designing Stable Layered Cathode Material for Sodium Ion Batteries Using Aluminum Doping, *J. Phys. Chem. Lett*. **2017**, *8*, 5021-5030.

[44a]R. Zhao, J. Liang, J. Huang, R. Zeng, J. Zhang, H. Chen, G. Shi, Improving the Ni-rich $LiNi_{0.5}Co_{0.2}Mn_{0.3}O_2$ properties at high operating voltage by double coating layer of Al_2O_3 and $AlPO_4$, *J. Alloy and Comp*, **2017**, *724*, 1109-1116.

[44b]D. Aurbach, K. Gamolsky, B. Markovsky, G. Salitra, Y. Gofer, U. Heider, R. Oesten, M. Schmidt, *Journal of the Electrochemical Society*, **2000**, *147(4)*, 1322-1331.

[45] H. Wang, Y. I. Jang, B. Huang, D. R. Sadoway, Y. M. Chiang, TEM Study of Electrochemical Studying Induced Damage and Disorder in $LiCoO_2$ Cathodes for Rechargable Lithium Batteries, *Journal Of the Electrochemical Society*, **1999**, *146(2)*, 473-480.

[46] L. Chen, R. E. Warburton, K. Chen, J. A. Libera, C. Johnson, Z. Yang, M. C. Hersam, J. P. Greeley, J. W. Elam, Mechanism for Al_2O_3Atomic Layer Deposition on $LiMn_2O_4$ from In-Situ Measurements and Ab-Initio Calculations, *Chem*, **2018**, *4*, 1-18.